Petroleum Science 21 (2024) 2650–2662

Contents lists available at ScienceDirect

Petroleum Science

journal homepage: www.keaipublishing.com/en/journals/petroleum-science

Original Paper

Development and performance evaluation of high temperature resistant strong adsorption rigid blocking agent

Zhe Xu [a], Jin-Sheng Sun [a, b, *], Jing-Ping Liu [a, **], Kai-He Lv [a], Xiao-Dong Dong [a], Zong-Lun Wang [a], Tai-Feng Zhang [a], Yuan-Wei Sun [a], Zhi-Wen Dai [a]

[a] School of Petroleum Engineering, China University of Petroleum (East China), Qingdao, 266580, Shandong, China
[b] CNPC Engineering Technology R&D Company Limited, Beijing, 102206, China

ARTICLE INFO

Article history:
Received 10 September 2023
Received in revised form
20 March 2024
Accepted 25 March 2024
Available online 26 March 2024

Edited by Jia-Jia Fei

Keywords:
High adsorption
Rigid microsphere
High temperature resistance
Blocking performance

ABSTRACT

As drilling wells continue to move into deep ultra-deep layers, the requirements for temperature resistance of drilling fluid treatments are getting higher and higher. Among them, blocking agent, as one of the key treatment agents, has also become a hot spot of research. In this study, a high temperature resistant strong adsorption rigid blocking agent (QW-1) was prepared using KH570 modified silica, acrylamide (AM) and allyltrimethylammonium chloride (TMAAC). QW-1 has good thermal stability, average particle size of 1.46 μm, water contact angle of 10.5°, has a strong hydrophilicity, can be well dispersed in water. The experimental results showed that when 2 wt% QW-1 was added to recipe A (4 wt % bentonite slurry+0.5 wt% DSP-1 (filtration loss depressant)), the API filtration loss decreased from 7.8 to 6.4 mL. After aging at 240 °C, the API loss of filtration was reduced from 21 to 14 mL, which has certain performance of high temperature loss of filtration. At the same time, it is effective in sealing 80–100 mesh and 100–120 mesh sand beds as well as 3 and 5 μm ceramic sand discs. Under the same conditions, the blocking performance was superior to silica (5 μm) and calcium carbonate (2.6 μm). In addition, the mechanism of action of QW-1 was further investigated. The results show that QW-1 with amide and quaternary ammonium groups on the molecular chain can be adsorbed onto the surface of clay particles through hydrogen bonding and electrostatic interaction to form a dense blocking layer, thus preventing further intrusion of drilling fluid into the formation.

1. Introduction

With the current rapid expansion and increase in China's demand for oil and natural gas, crude oil's dependence on the outside world is increasing year by year. It has reached 70.9% in 2022, well above the internationally recognised safety threshold of 50%. Natural gas external dependence reaches 42.5% in 2022. Deep and ultra-deep oil and gas resources are abundant, and are the most realistic replacement energy source for China. China's total deep and ultra-deep oil and gas resources amount to 67.1 billion tonnes of oil equivalent, accounting for 34% of the country's total oil and gas resources. Deep and ultra-deep layers have become the main position for major oil and gas discoveries in China, and accelerating deep oil and gas exploration and development has also become an inevitable choice for guaranteeing national energy security. With the increase of reservoir depth, the complexity of formation and pressure system, high temperature and high pressure and high geostress bring great challenges to drilling (Guo et al., 2020; Wang et al., 2022). Among them, drilling fluid is one of the core engineering technologies for deep and ultra-deep well drilling, which is the key to ensure the success of drilling (Feng et al., 2020; Gautam et al., 2022; Lou et al., 2022; Xu et al., 2022). However, the intrusion of drilling fluid into the formation causes hydration of clay particles, leading to downhole accidents, seriously affecting the efficiency of well construction and even preventing well completion. Therefore, strengthening the sealing ability of drilling fluids and stopping the intrusion of drilling fluids is the key to stabilising the well wall.

It is well known that inorganic materials are widely used in

* Corresponding author.
** Corresponding author.
E-mail addresses: sunjsdri@cnpc.com.cn (J.-S. Sun), liujingping20@126.com (J.-P. Liu).

https://doi.org/10.1016/j.petsci.2024.03.021

drilling fluids due to their advantages of good temperature resistance, high strength, and wide material sources (Bai et al., 2021; Ismail et al., 2016; Villada et al., 2022). Mainly include: silica and its modified products, calcium carbonate, nano Fe_3O_4, etc. Among them, silica has high thermal stability and can keep its physical and chemical properties stable in high-temperature environments. Meanwhile, silica has high mechanical strength and hardness, which makes it exhibit good wear, pressure and impact resistance in material processing and engineering applications (Boyou et al., 2019; Kök and Bal, 2019). Due to the presence of a large number of hydroxyl groups (−OH) on the surface of silica, it is easy to absorb water and cause agglomeration, thus limiting the application of silica, and it is usually necessary to modify the surface of silica. Silica modified by coupling agents (vinyltrimethoxysilane (VTMS), γ-methacryloyloxypropyltrimethoxysilane (KH570), etc.) not only has improved dispersion. It also has a carbon-carbon double bond and can copolymerise with polymerisation monomers. The thermal stability of silica can be utilized to improve the temperature resistance of the copolymer to some extent. Therefore, the development of polymer/silica composites has become a hotspot in recent years to overcome the high temperature failure of drilling fluid treatments.

Liu et al. (2021) used VTMS for surface modification of silica and grafted N, N-dimethylacrylamide (DMAA) and 2-acryloylamino-2-methyl-1-propanesulfonic acid (AMPS) on the surface to obtain a filter loss depressant (NS-DA). NS-DA is resistant to temperatures up to 180 °C. After high temperature action, the filtration loss of drilling fluid with NS-DA added was only 5.6 mL at medium pressure (0.7 MPa). Li et al. (2023) grafted acrylamide (AM), AMPS and N-vinyl caprolactam (NVCL) onto KH570-modified silica nanoparticles to obtain a water-based drilling fluid filter loss reducer (AAN-g-SiO_2), which is temperature resistant up to 220 °C. Mao et al. (2015) synthesized polymeric silica nanocomposites (SDFL) by reacting AM, AMPS, styrene (St) with silica nanocomposites. The material is resistant to temperatures up to 230 °C, which significantly reduces the loss of filtration and improves the pressure-bearing capacity of the formation. Ao et al. (2021) prepared an amphiphilic silica-based inorganic/organic hybrid material (ZSHNM) by polymerisation of AMPS, N-vinylpyrrolidone (NVP) and a cationic monomer (dimethyldiallylammonium chloride, DMDAAC) with silica bearing vinyl groups on the surface. ZSHNM has a good filtration loss reduction effect even at 240 °C. Martin et al. (2023) modified silica using a cationic surfactant (cetyltrimethylammonium bromide) to give good high temperature stability both at 149–232 °C. The author also developed a blocking agent (PANS) that can resist temperatures up to 180 °C using silica polymerised with other monomers in preliminary experiments (Xu et al., 2023).

Numerous studies have shown that the introduction of silica and modified silica improves the temperature resistance of polymers. Meanwhile, cationic nanosilica has better blocking effect than anionic nanosilica. The introduction of cationic monomer makes the prepared treatment agent positively charged, which can be adsorbed onto clay particles (negatively charged) under the action of electrostatic gravity, forming a dense mud cake and preventing the drilling fluid from intruding into the formation. Among them, quaternary ammonium cations have strong temperature resistance and resistance to inorganic ion contamination, making them commonly used as synthetic temperature- and salt-resistant drilling fluid treatments (Cescon et al., 2018; Hoxha et al., 2019; Yu, 2015).

Therefore, in this paper, a temperature-resistant adsorbent rigid blocking agent (QW-1) was developed by using the thermally stable and rigid KH570-modified silica (KH570—SiO_2), the cationic monomer allyltrimethylammonium chloride (TMAAC) with a short molecular chain, and AM as the polymerisation monomer.

2. Experimental section

2.1. Experimental materials

Acrylamide (AM), allyltrimethylammonium chloride (TMAAC), and silica (5 μm) were obtained from Aladdin Biochemical Technology Co. KH570—SiO_2 was purchased from Andy's Metal Materials Ltd. KH570—SiO_2 has an average particle size of about 1 μm and is hydrophobic. Anhydrous ethanol, anhydrous calcium carbonate, sodium chloride (NaCl) and potassium persulfate (APS) were purchased from Sinopharm Chemical Reagent Co. Ltd (China). Calcium carbonate (2.6 μm) was purchased from Changxing Qingsheng Calcium Co. Ltd (China). DSP-1 (Filtration Loss Reducer) was purchased from Desunyuan Petroleum Technology Co. (China). All other chemicals used are of analytical grade and do not require further purification.

2.2. Preparation of strong adsorption rigid blocking agent

First, a certain amount of KH570—SiO_2 was added to anhydrous ethanol for dispersion. Then, AM (5 g) and TMAAC (3 g) were added to water and stirred until dissolved. Then, the above two liquids were added to the three-necked flask sequentially. The rotational speed was set to 350 r/min, the water bath was heated to 60 °C, and nitrogen was passed for 30 min. Then, APS (0.1 g) was dissolved in water (2 g) and added dropwise into a three-necked flask using a dropper for 5 h. The reaction was carried out. Finally, the obtained product was kept in a glass bottle for reserve, which was named QW-1. The synthetic schematic of QW-1 is shown in Fig. 1.

2.3. Characterisation method

QW-1 was purified with anhydrous ethanol and dried by drying oven. Grinding was carried out using an agate mortar to obtain the sample to be tested. An infrared spectrometer (IRTrancer-100, Shimadzu, Japan) was used to study the molecular structure of the strongly adsorbed rigid blocking agent QW-1 with a resolution of 4 cm^{-1} and a wavelength range of 4000–400 cm^{-1}. The thermal stability analysis of QW-1 was carried out under nitrogen protective atmosphere in the temperature range of 40–800 °C at a heating rate of 10 °C/min^{-1}, using a thermogravimetric analyser (TGA, Mettler Toledo, USA).

The solid particles obtained above were dispersed into water and sonicated for 10 min. Scanning electron microscopy (SEM) and transmission electron microscopy (TEM) were used to observe the QW-1 microscopic morphology.

The particle size distribution of QW-1 in water was determined by laser particle sizer (Malvern, UK). Disperse QW-1 in water, add drops to the slide with a dropper, and then dry, repeating several times so that QW-1 is evenly dispersed on the slide. The water contact angle of QW-1 was determined by optical contact angle measuring instrument (OCA25). Weigh 0.2 g of QW-1 powder in a glass bottle, add 20 mL of water and sonicate for 30 min to observe its dispersion in water.

2.4. Performance evaluation methods

Since QW-1 was a cationic blocking agent, the drilling fluid formulation chosen for this experiment was 4 wt% bentonite

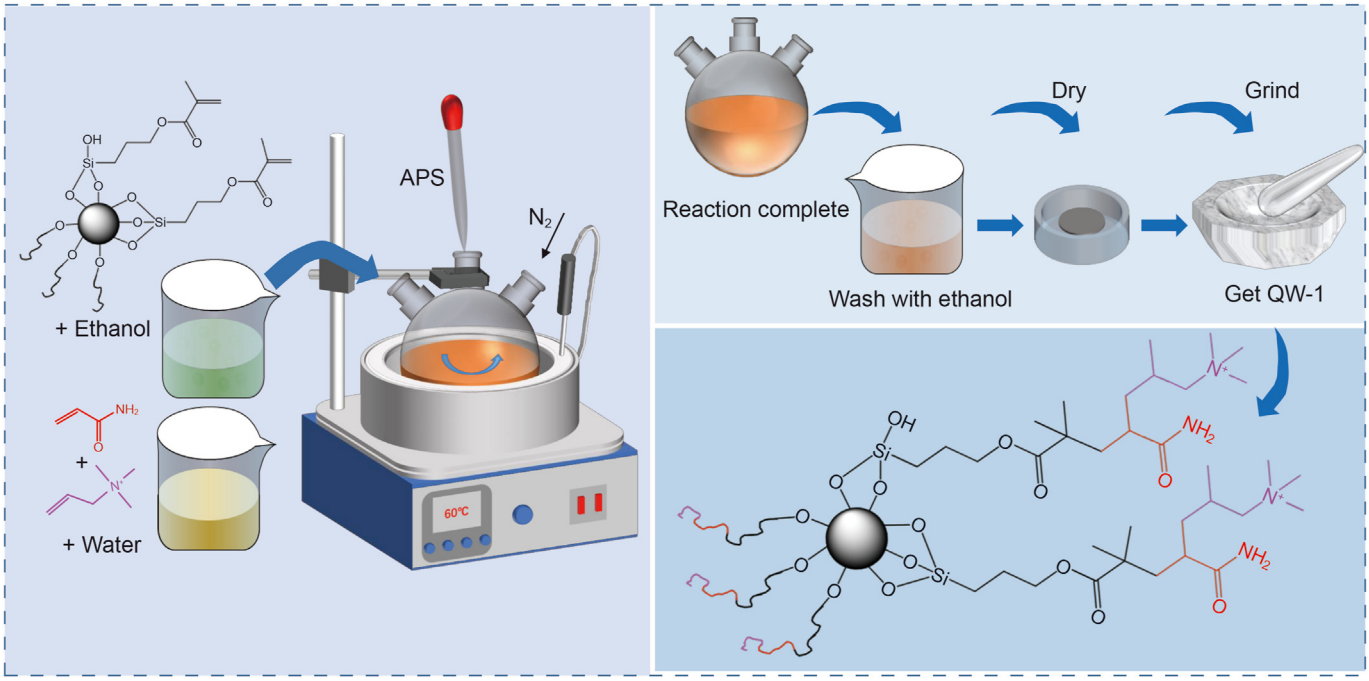

Fig. 1. Schematic of the synthesis of QW-1.

slurry+0.5 wt% DSP-1. DSP-1 can increase the viscosity of bentonite slurry, prevent the aggregation and deposition of clay particles, improve the stability of bentonite slurry and reduce the amount of filtration loss. 16 g bentonite and 1.2 g anhydrous sodium carbonate were added sequentially under stirring conditions in 400 mL of water, stirred at high speed for 30 min, and then sealed and maintained for 24 h. 4 wt% bentonite slurry was obtained. The drilling fluid used in the experiment was obtained by adding 0.5 wt % DSP-1 to 4 wt% bentonite slurry (noted as recipe A).

Different amounts of QW-1 were added to recipe A. The rheological, filtration loss and blocking properties of the drilling fluids before and after aging were determined by using a six-speed rotational viscometer, API medium-pressure filtration loss meter, high-temperature and high-pressure (HTHP) filtration loss meter, and sand-bed blocking meter.

2.5. Mechanism of action evaluation methods

Take 2 g of bentonite in deionized water and different concentrations of QW-1 dispersions and stir well at room temperature until well mixed. It was left for 24 h to make the adsorption sufficient. The precipitate was washed multiple times and then dried in an oven. Infrared spectroscopy was used to determine the structural changes in the clay after the action of QW-1. Changes in the spacing of bentonite crystal layers were characterized by X-ray diffractometry (XRD, X'pert PRO MPD), experimentally using a Cu target with a scanning range of 4°–13°. Thermal decomposition of QW-1 treated bentonite was studied by thermogravimetric analyser.

Weigh 6 g of QW-1 into 200 mL of deionized water and slowly add 5 g of bentonite during mixing. Stir at 5000 r/min for 20 min to ensure that the bentonite was well dispersed in the solution. The mixture was kept airtight and allowed to stand for 24 h in a thermostat at 30 ± 1 °C. The mixture was then stored in a sealed container. The rested mixture was filtered and the content of various cations (Ca^{2+}, Mg^{2+}, Na^{+}) in the filtrate was determined by ICP. A blank control test was also done, i.e., only 5 g of bentonite was added to 200 mL of deionized water to determine the content of various cations in the filtrate after the same operation.

The dispersion solution of QW-1 was prepared, and the shale flakes were suspended in the dispersion solution and left to stand for 24 h. The shale flakes were then dried in an oven at 105 °C. Remove the shale flakes, rinse with water, and place them in an oven at 105 °C for drying. The adsorption of QW-1 on the surface of shale flakes was observed by scanning electron microscopy. The mud cake formed after API filtration loss was placed in an oven at 105 °C for drying. The blocking of QW-1 was observed by scanning electron microscopy.

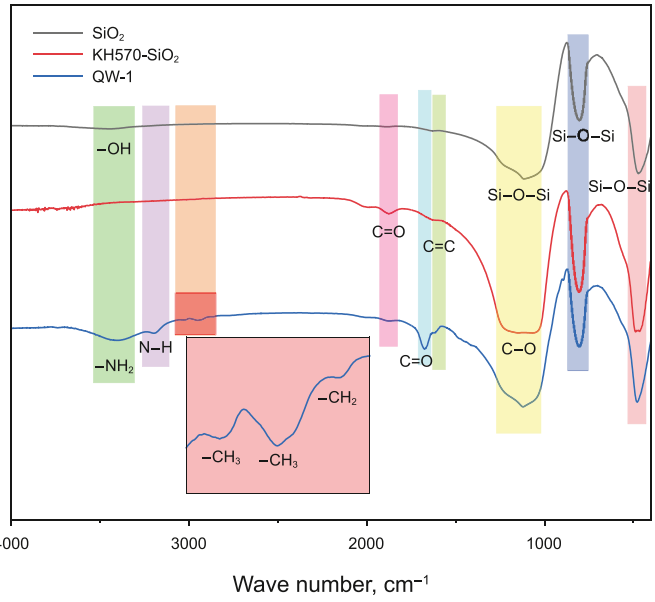

Fig. 2. Infrared spectra of QW-1.

3. Analysis and evaluation

3.1. Characterisation

3.1.1. Infrared spectral analysis

Fig. 2 shows the infrared spectral analysis of SiO_2, KH570–SiO_2, and QW-1. On the infrared spectrogram of SiO_2, the stretching vibration of –OH appeared at 3446 cm^{-1}; the antisymmetric stretching vibration peak of Si–O–Si at 1120 cm^{-1}; the symmetric stretching vibration peak of Si–O–Si at 806 cm^{-1}; and bending stretching vibratio peak of Si–O–Si at 476 cm^{-1} (Luz et al., 2019; Wang Y.T. et al., 2023; Yu et al., 2020). After the modification of SiO_2 by KH570, new absorption peaks appeared near 1836 and 1637 cm^{-1}, the stretching vibration peak of the C=O group in KH570. Meanwhile, a C–O stretching vibration peak existed in the range of 1200–1000 cm^{-1}. It showed that KH570 has been grafted onto SiO_2 (Jiang et al., 2017). In contrast to KH570-modified SiO_2, QW-1 showed a $-NH_2$ stretching vibration peak at 3396 cm^{-1}. The N–H stretching vibration peak on the amide group at 3196 cm^{-1}. The $-CH_3$ deformation stretching vibration peak on the quaternary ammonium group appeared at 3028 cm^{-1}. The $-CH_3$ stretching vibration peak at 2951 cm^{-1}. The $-CH_2$ stretching vibration peak at 2868 cm^{-1}. 1672 cm^{-1} for the stretching vibration peak of the C=O group (Jia et al., 2022; Shen et al., 2023). The results showed that the characteristic peaks related to AM, TMAAC, and modified SiO_2 were reflected in the infrared spectrograms of the products, which verified that the product molecular chain had a designed molecular structure.

3.1.2. TGA analysis

Fig. 3 shows the thermogravimetric curve of QW-1. From the curves, it can be seen that the thermal decomposition of QW-1 is roughly divided into the following stages. The weight loss of QW-1 before 247 °C was 0.7%. Heat loss in the range of 40–247 °C is mainly volatilization of adsorbed water from the sample. Little thermal decomposition of molecular chains occurs at this stage. Therefore, the samples have a certain resistance to temperature until 247 °C. Thermal decomposition of the branched chains of the molecular chain was initiated at 247–331 °C with a weight loss of 3.1%. Of these, the main ones are amide groups, quaternary ammonium groups, and the decomposition of methyl groups. When the temperature is higher than 337 °C, the main chain of QW-1 starts to undergo thermal decomposition. From the thermogravimetric curve, it can be seen that the sample was only thermally decomposed by about 3% before 300 °C, indicating that QW-1 has good thermal stability.

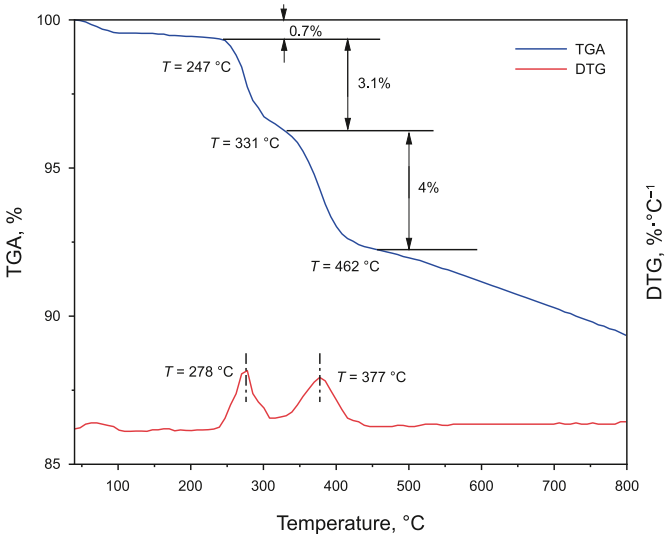

Fig. 3. Thermogravimetric curve of QW-1.

3.1.3. SEM and TEM analysis

Fig. 4 shows the SEM (Fig. 4(a)) and TEM (Fig. 4(b)) of QW-1 after dispersion in clear water. As shown in Fig. 4(a), QW-1 was spherical in shape, and all particles maintained a good monodispersity with a homogeneous particle size distribution. The dispersion in water was good, no agglomeration, and the particle size was about 1 μm. Meanwhile, Fig. 4(b) further confirms the authenticity of SEM. It can be observed on the TEM image that the QW-1 particle size is consistent with the SEM-determined particle size.

3.1.4. Particle size analysis

Fig. 5 shows the particle size distribution of QW-1 in water. The average particle size of QW-1 is 1.46 μm, which is slightly larger than that tested by SEM and TEM. This may be due to the presence of hydrophilic groups (amide groups) on the surface of QW-1, which can absorb water in aqueous environments, placing QW-1 in a state of being dissolved by water. During SEM and TEM experiments, due to the need to dry the samples first and the bombardment of high-speed electrons under high vacuum conditions, the water in QW-1 volatilized, causing the particles to shrink.

3.1.5. Dispersibility analysis in water

The water contact angle and dispersion of QW-1 in water are shown in Fig. 6. From Fig. 6(a), the water contact angle of QW-1 is 10.5°. Hydrophilic groups were introduced during the synthesis of QW-1 to give it a better hydrophilicity. It can be observed from Fig. 6(b) that QW-1 can be well dispersed in water to form a milky suspension. It is because of the amide group and quaternary ammonium group grafted on the surface of QW-1, which can form hydrogen bond with water molecules and enhance hydrophilicity, so it can be dispersed in water to form a suspension.

3.2. Performance evaluations

3.2.1. Effect of dosage on drilling fluid performance

Different amounts of QW-1 were added to recipe A to determine the rheological and leaching properties, and the test results are shown in Fig. 7. As shown in the figure, the apparent viscosity (AV), plastic viscosity (PV) and dynamic shear force (YP) of the drilling fluid change less with the increase of QW-1 concentration, indicating that QW-1 has less influence on the rheological properties of the drilling fluid. Drilling fluid filtration loss decreases with increasing QW-1 concentration. At a concentration of 2 wt%, the filtration loss was reduced from 7.8 to 6.4 mL. The performance was better at this concentration and therefore, this concentration was chosen for the next experiments.

3.2.2. Temperature resistance

As the scope of oil and gas exploration and development is gradually moving towards the deep ultra-deep layer, the high temperature stability performance of the drilling fluid treatment agent puts forward higher requirements. Therefore, the temperature stability performance of QW-1 was experimentally evaluated. 2 wt% of QW-1 was added to the drilling fluid to determine the rheological and filtration loss properties of the drilling fluid after aging at different temperatures, and the experimental results are shown in Fig. 8. As shown in the figure, the rheological properties of the drilling fluid change a lot before and after aging, which is partly mainly due to the thermal degradation of DSP-1 under the action of high temperature, resulting in the reduction of the viscosity of the

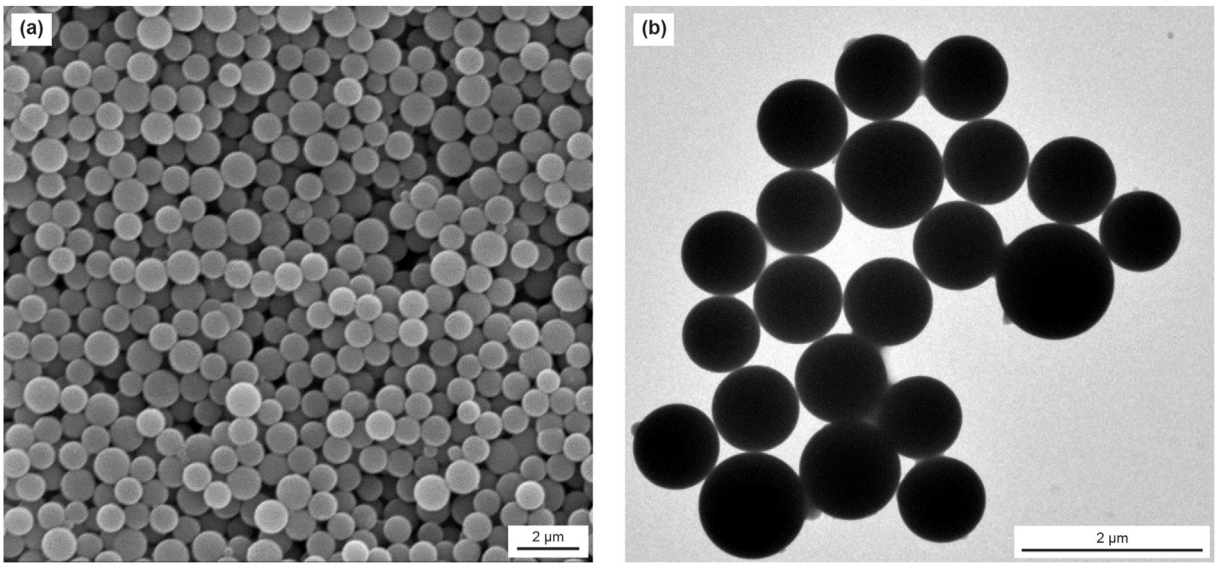

Fig. 4. Microscopic morphology of QW-1.

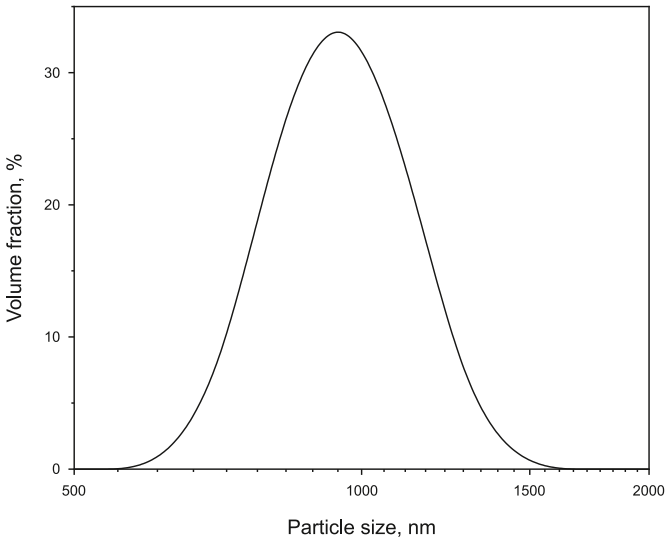

Fig. 5. Particle size distribution of QW-1.

drilling fluid. With the increase of QW-1 concentration in the drilling fluid, the apparent viscosity changes before and after the aging of the drilling fluid at 200–260 °C were small, which indicated that QW-1 had little effect on the rheological properties of the drilling fluid. It was because QW-1 was a low molecular weight rigid blocking agent, which had less influence on the rheological properties of the drilling fluid due to its low molecular weight. After aging at 240 °C for 16 h, the filtration loss of drilling fluid without QW-1 was 21 mL. When QW-1 was spiked at 2 wt%, the loss on filtration was 14 mL. It shows that QW-1 can still further reduce the filtration loss of drilling fluid at high temperature.

3.2.3. Salt resistance

Fig. 9 shows the apparent viscosity and filtration loss properties of drilling fluids with recipe A and recipe A+2 wt% QW-1 before and after aging at 240 °C under different NaCl concentrations, respectively. As shown in Fig. 9(a), the trends of apparent viscosities of drilling fluids without QW-1 and with QW-1 at different NaCl concentrations were similar. As shown in Fig. 9(b), the filtration loss of drilling fluid increased with the increase of NaCl concentration, and the addition of QW-1 could further reduce the filtration loss of

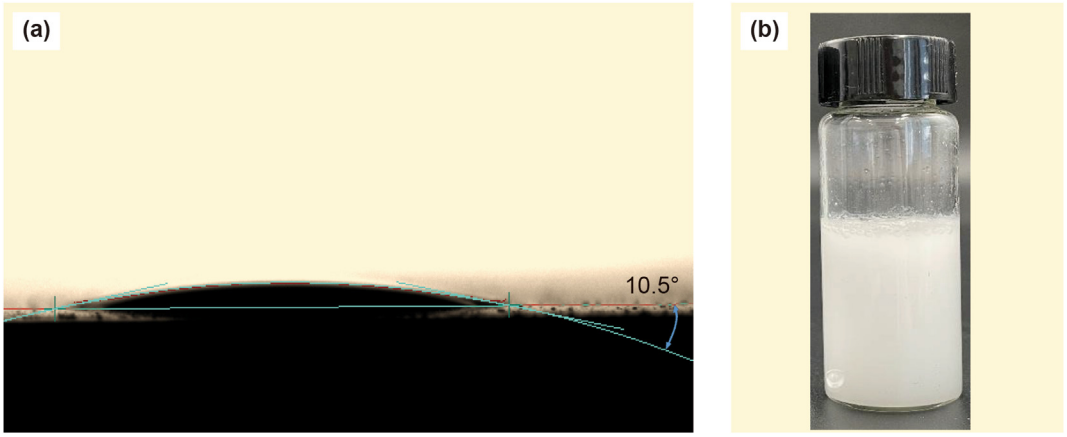

Fig. 6. Water contact angle and dispersion in water of QW-1.

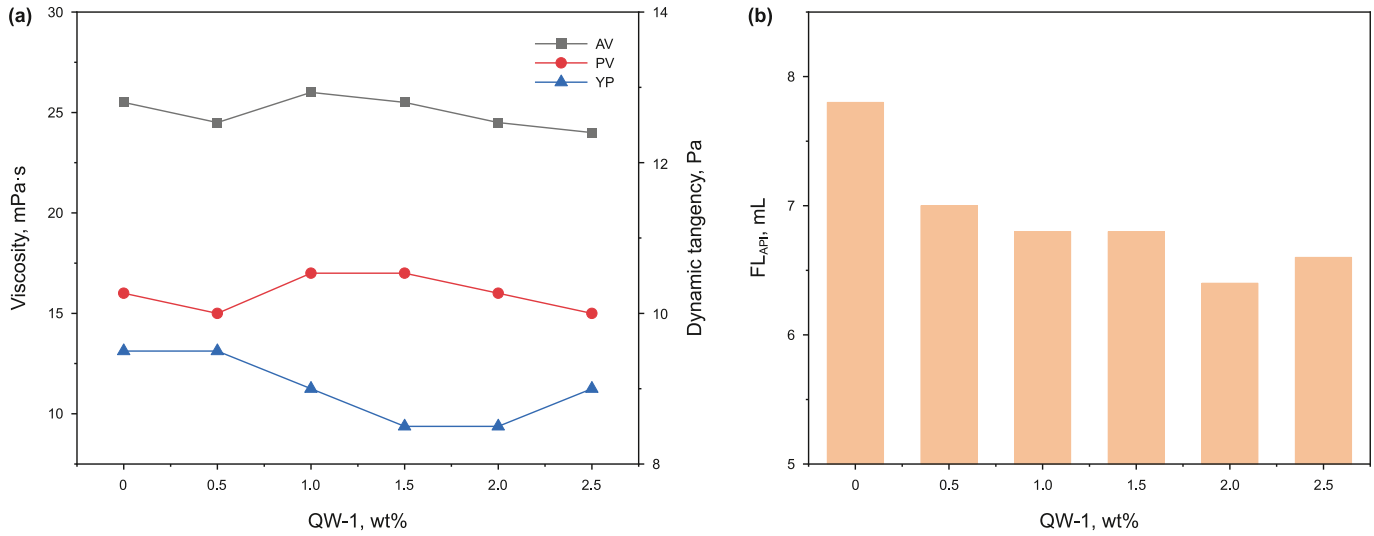

Fig. 7. Effect of QW-1 concentration on drilling performance.

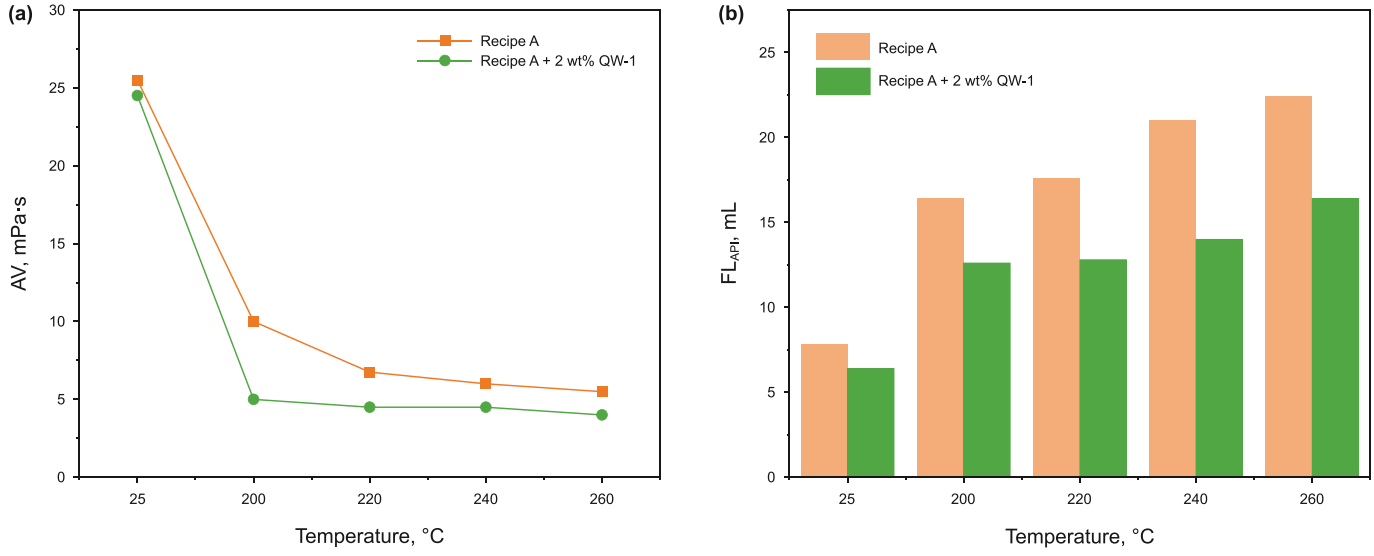

Fig. 8. Effect of temperature on drilling performance.

drilling fluid. When the NaCl concentration was 15 wt%, the filtration loss before and after aging of drilling fluid without QW-1 was 25.6 and 83.4 mL, respectively. And the filtration loss before and after adding QW-1 drilling fluid aging were 14.8 and 68.8 mL, respectively. Before the NaCl concentration of 15 wt%, the filtration loss before and after aging of drilling fluid was relatively low. This suggests that QW-1 can play a role in reducing the filtration loss under ultra-high temperature and high salt conditions.

3.2.4. Sand bed plugging performance

Using visualised medium-pressure sand bed plugging filtration loss apparatus, the permeability sand bed plugging performance of commonly used domestic and foreign treating agents (SiO_2, $CaCO_3$) was evaluated in comparative experiments using 80–100 mesh and 100–120 mesh sand beds as the evaluation media, and the experimental results are shown in Fig. 10. The shallower the depth of sand bed intrusion, the better the sealing of the blocking agent. As shown in the figure, for recipe A, the addition of the blocking agent significantly reduces the depth of intrusion into the sand bed. The 80–100 mesh sand bed was intruded at a depth of 10.8 cm for recipe A. The depth of intrusion of the drilling fluid with SiO_2 and $CaCO_3$ added was 5.6 and 6.5 cm, respectively. In contrast, the depth of drilling fluid intrusion was significantly reduced to 3.9 cm with the addition of QW-1. Similarly, for the 100–120 mesh sand bed, the depth of intrusion for recipe A was 9.4 cm. The depth of intrusion of the drilling fluid with SiO_2 and $CaCO_3$ added was 4.2 and 5.1 cm, respectively. However, the depth of drilling fluid intrusion with the addition of QW-1 was 2.6 cm. This is mainly due to the presence of a large number of cationic groups on the surface of QW-1, which can be adsorbed on the surface of quartz sand through electrostatic action. And it bridges the gap before the sand grains to form a blocking layer, preventing the drilling fluid from further intruding into the sand bed.

3.2.5. Ceramic sand disc blocking performance

The ceramic sand disc blocking experiment is mainly to determine the amount of filtration loss of drilling fluid in 30 min after aging at 240 °C under the condition of temperature 200 °C and

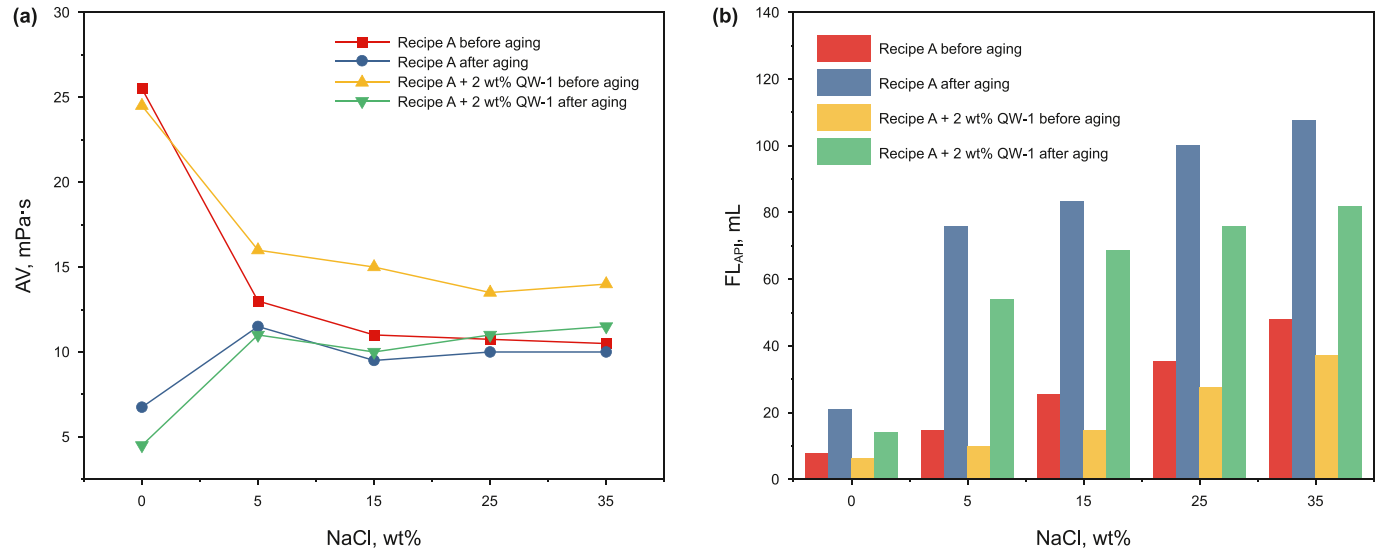

Fig. 9. Effect of NaCl concentration on drilling performance.

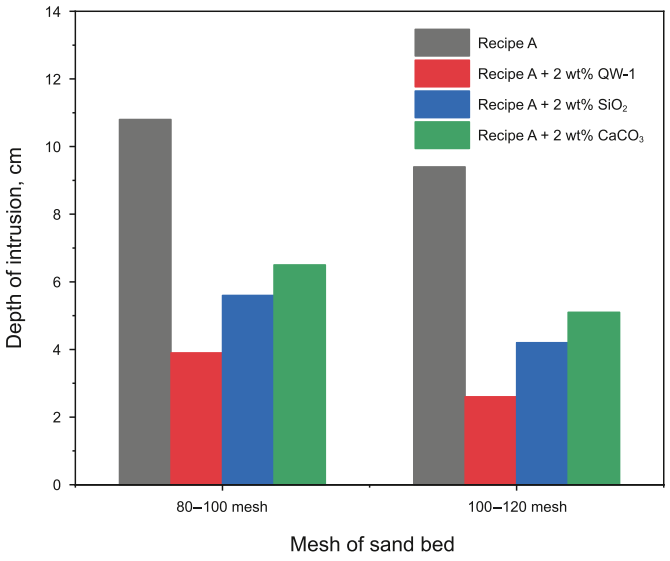

Fig. 10. Experimental results of sand bed blocking.

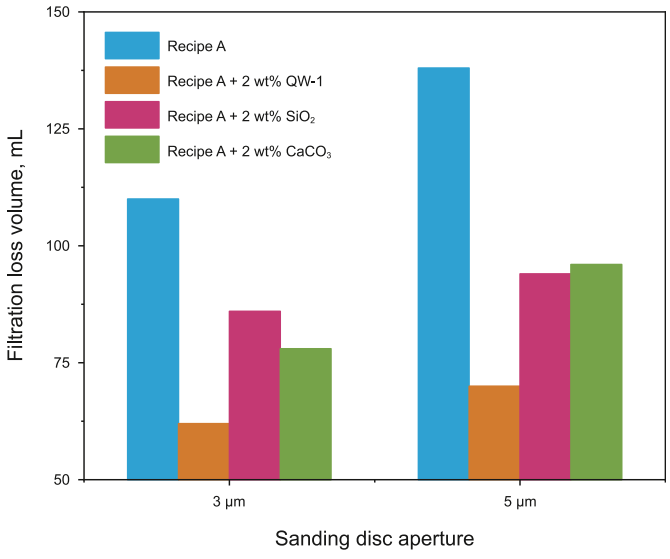

Fig. 11. Experimental results of ceramic sand disc blocking.

differential pressure 3.5 MPa, and the experimental results are shown in Fig. 11. For 3 and 5 μm sand discs, the sand disc filtration loss for recipe A was 110 and 138 mL, respectively. After adding 2 wt % QW-1, the sand disc filtration loss of drilling fluid was reduced to 62 and 70 mL, respectively, and was significantly lower than the sand disc filtration loss of SiO_2 and $CaCO_3$ at the same dosage. Meanwhile, the sand disc filtration loss was reduced by 43.6% and 49.3%, respectively, compared to recipe A. Experiments show that QW-1 can effectively seal the pores of sand discs under high temperature and high pressure conditions, thus effectively reducing the filtration loss of drilling fluid and having good sealing performance.

3.3. Mechanism of action analysis

3.3.1. Infrared spectral analysis

The results of infrared analysis of bentonite before and after interaction with QW-1 are shown in Fig. 12. As can be seen from the figure, both bentonite and bentonite treated with QW-1 produced infrared absorption peaks at wavelengths of 3624, 1645, 1037, 914, 794, and 625 cm^{-1}, which belong to the typical absorption peaks of sodium-montmorillonite (Dong et al., 2019, 2022; Sun et al., 2022). Among them, 3624 cm^{-1} is the peak of stretching vibration of Al–OH in aluminium-oxygen octahedron. 1645 cm^{-1} is the peak of bending vibration of H–OH. 1037 cm^{-1} is the stretching vibration of Si–O–Si bond and Si–O bond. 914 cm^{-1} is the peak of infrared characteristics of Al–Al–OH. 794 cm^{-1} is the peak of Si–O stretching vibration. This indicates that the silicate skeleton of montmorillonite did not change after QW-1 treatment. The $-NH_2$ stretching vibration peak appears at 3396 cm^{-1}. 3196 cm^{-1} is the N–H stretching vibration peak on the amide group. 3028 cm^{-1} is the $-CH_3$ deformation stretching vibration peak on the quaternary ammonium group. 2951 cm^{-1} is the $-CH_3$ stretching vibration peak. 2868 cm^{-1} is the $-CH_2$ stretching vibration peak. 1672 cm^{-1} is the stretching vibration peak on the C=O group. The antisymmetric stretching vibration peak of Si–O–Si is at 1120 cm^{-1}. All

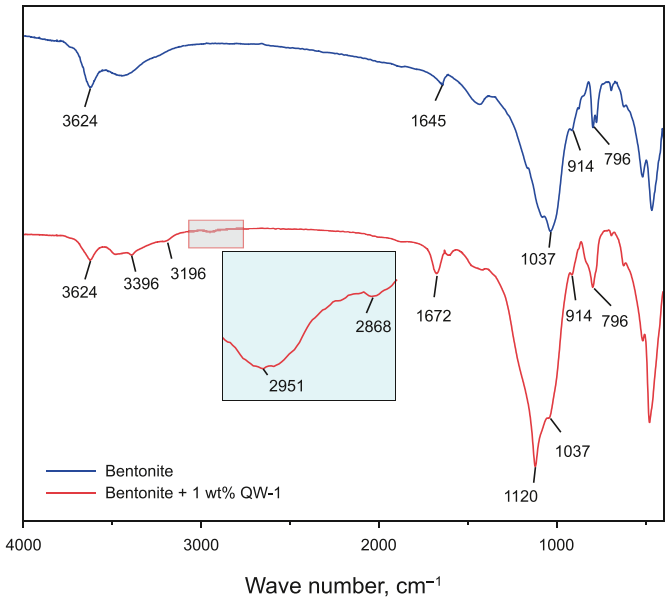

Fig. 12. Infrared spectra of bentonite before and after QW-1 treatment.

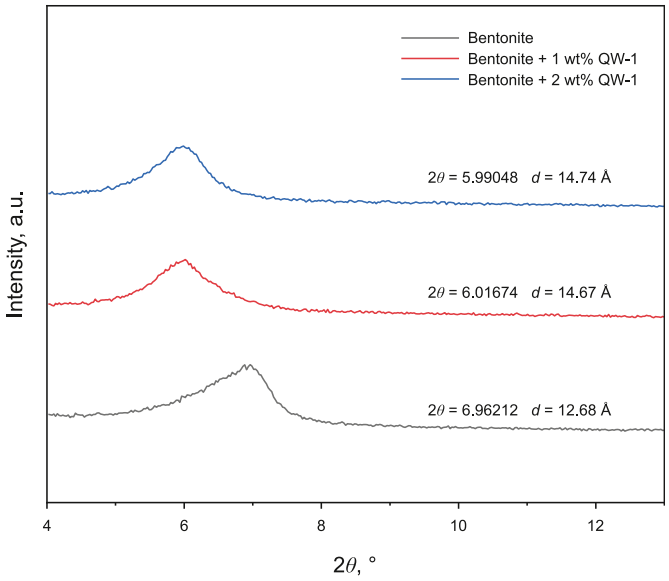

Fig. 13. XRD graph of bentonite before and after QW-1 treatment.

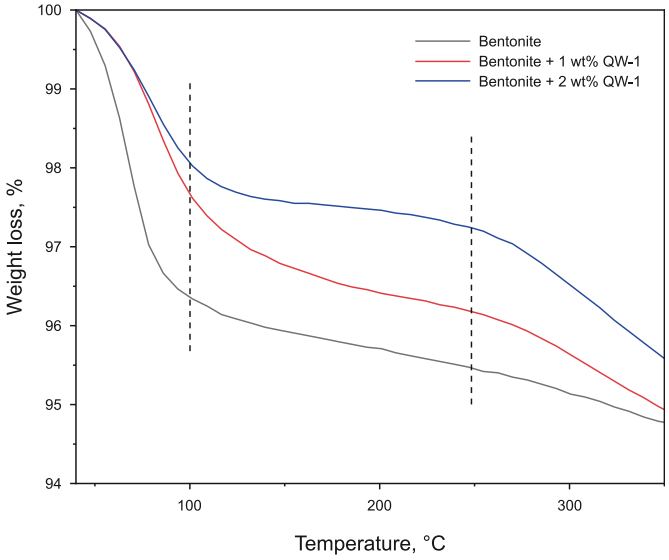

Fig. 14. TGA curves of bentonite before and after QW-1 treatment.

these absorption peaks belong to QW-1 synthesized in this paper, which indicates that QW-1 undergoes strong adsorption with bentonite. It is also complemented by the results of the QW-1 infrared analysis.

3.3.2. XRD analysis

Clay minerals have a lamellar crystalline structure. In the case of montmorillonite, for example, the cell in its crystal structure is composed of two layers of Si–O tetrahedra and one layer of Al–O octahedra. When clay minerals are exposed to water, water molecules will enter the clay mineral crystal layer, leading to changes in the spacing of the crystal layers. XRD can measure the montmorillonite d001 spacing by the diffraction angle formed when X-rays are irradiated onto the montmorillonite. Specifically, it is calculated by Bragg's formula: $2d\sin\theta = n\lambda$. Where: d is the crystal layer spacing (Å); θ is the diffraction angle (°); n is the refractive angle, which takes the value of 1; and λ is the wavelength of X-rays (nm).

The adsorption of QW-1 on bentonite is mainly by electrostatic attraction. This electrostatic action occurs through protonated amines exchanging out montmorillonite interlayer cations. This exchange inevitably leads to a certain change in the layer spacing, which can be further confirmed by XRD experiments. Fig. 13 shows the XRD spectrum of dry bentonite after treatment with water and different concentrations of QW-1. From the figure, it can be seen that the crystal layer spacing of the original bentonite is 12.68 Å in the dry state. The crystal layer spacing of bentonite gradually increases with increasing QW-1. The crystal layer spacing of bentonite was 14.74 Å when QW-1 was added at 2 wt%. This indicates that the molecular chains on QW-1 entered the bentonite interlayer and interacted with the negative charges on the bentonite surface to form a chemisorption layer, resulting in an increase in the spacing of the bentonite crystal layers (Dong et al., 2023; Luo et al., 2023; Wang Z.L. et al., 2023).

3.3.3. TGA analysis

In order to assess the effect of QW-1 on the clay, TGA was used to study the thermal decomposition of QW-1 treated bentonite, and the experimental results are shown in Fig. 14. The thermal decomposition temperature of QW-1 is 247 °C from Fig. 3. From Fig. 14, it can be seen that the temperature from 40 to 100 °C, the fastest heat loss was observed for the bentonite treated with water, with a loss rate of 3.8%. Only 0.8% was lost from 100 to 247 °C, which indicates that some water was adsorbed on the surface and interlayers of the bentonite treated with fresh water and was removed before 100 °C. The weight loss of the QW-1 treated bentonite was significantly less than that of the original bentonite up to 247 °C. The weight loss of the bentonite from the 1 wt% QW-1 treatment was 3.9%. The weight loss of the bentonite from the 2 wt % QW-1 treatment was 1.8%. This indicates that the addition of QW-1 resulted in fewer water molecules adsorbed by the bentonite, which in turn suggests that the hydration and swelling of the clay surface is weak. Figs. 13 and 14 indicate that QW-1 can be adsorbed

Table 1
ICP ion concentration measurement results.

Type	Ion concentration in solution before exchange, mg/L			Ion concentration in solution after exchange, mg/L		
	Ca^{2+}	Mg^{2+}	Na^{+}	Ca^{2+}	Mg^{2+}	Na^{+}
Blank base slurry	3.13	0.23	324.68	–	–	–
QW-1 after treatment	5.58	0.71	453.5	2.45	0.48	128.82

on the surface of bentonite or into the interlayer, which hinders the entry of water molecules and retards the hydration and swelling of bentonite.

3.3.4. Cation exchange analysis

Montmorillonite is more negatively charged due to the presence of lattice substitutions, so the number of adsorbed cations around it is higher (mainly Na^{+}, Ca^{2+}), and the number of exchangeable cations is also higher, and the hydrated cations bring a thick hydration film to the clay, which makes the montmorillonite hydrated and swollen (Sun et al., 2019; Yi et al., 2016). The larger the ionic radius and the greater the charge, the greater the ion exchange capacity, irrespective of the ionic concentration. Table 1 shows the results of inductively coupled plasma (ICP) measurements. From the table, it can be seen that the blank base slurry filtrate has the highest concentration of Na^{+}, while the concentrations of Ca^{2+} and Mg^{2+} are relatively low, which indicates that the hydrated cations in the clay crystal layer are mainly Na^{+}. Therefore, this bentonite has strong hydration dispersion and swelling ability. After the addition of QW-1, the Na^{+} content increased significantly, indicating that the NH^{4+} in QW-1 exchanged the Na^{+} in the clay by cation exchange.

3.3.5. Adsorption on rocks

Fig. 15 shows the adsorption of QW-1 on shale sheets. In the figure, a large number of QW-1 particles are adsorbed at the cracks and pores of the shale sheet. As the rock surface is negatively charged, and QW-1 is a cationic blocking agent, it can have electrostatic adsorption effect with the rock surface. Through this action, QW-1 is firmly adsorbed on the rock surface and can fill in the cracks and pores to play the role of sealing.

3.3.6. Microscopic morphology of the mud cake

Fig. 16 shows the micro-morphology of drilling fluid mud cake after aging at different temperatures. Among them, Fig. 16(a), (c), (e), (g), (i) are SEM images of recipe A, and Fig. 16(b), (d), (f), (h), (j) are SEM images of recipe A+2 wt% QW-1. For recipe A, the surface of the mud cake was relatively flat at 25 °C, with no obvious cracks or pores. As the aging temperature increases, the high temperature effect causes clay particles to aggregate, resulting in cracks and pores on the surface of the mud cake. This is one of the reasons for the increase in filtration loss after high temperatures. However, the surface of the mud cake after adding QW-1 was flat, and no cracks or pores appeared on the surface as the temperature increased. The partially enlarged picture observes a large amount of QW-1 together with clay particles to form a mudcake skeleton, which stops the filtration loss of drilling fluid. Meanwhile, a large number of QW-1 microspheres still existed on the surface of the mud cake even after the action of high temperature at 260 °C, and the shape did not change. This shows that even at ultra-high temperatures, QW-1 still maintains the shape of the microspheres without destroying them, thus providing a sealing effect.

3.3.7. Microscopic morphology of sanding discs

Fig. 17 shows the SEM images of the 3 and 5 μm ceramic sand discs before and after blocking, respectively. From the figure, it can be seen that there are a large number of pores and cracks in the sand disc before blocking, leading to easy filtration of drilling fluid. Compared with the porous structure of the sand disc before blocking, the tiny pore slits of the sand disc after blocking are filled with a large number of nanoparticles, forming a denser blocking layer. This indicates that QW-1 effectively sealed the microporous seams of the sand disc.

3.3.8. Research on blocking mechanism

The blocking mechanism of strong adsorption rigid blocking agent QW-1 is shown in Fig. 18. QW-1 molecular chain with amide groups and quaternary ammonium groups, and clay particles in addition to hydrogen bonding force, but also through the principle of negative charge anisotropic charge attraction with the formation, so that the QW-1 particles adsorbed in the well wall clay particles and retained in the well wall. At the same time, particles of reasonable size enter the cracks, create adhesion and aggregate with each other to form an inner mud cake, establishing a dense

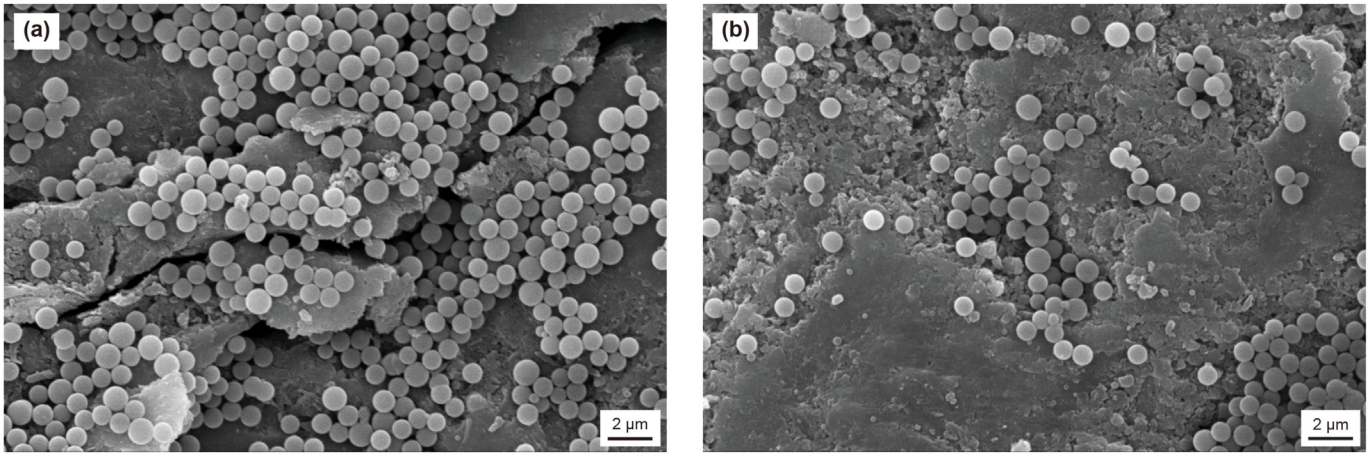

Fig. 15. Adsorption of QW-1 on rock.

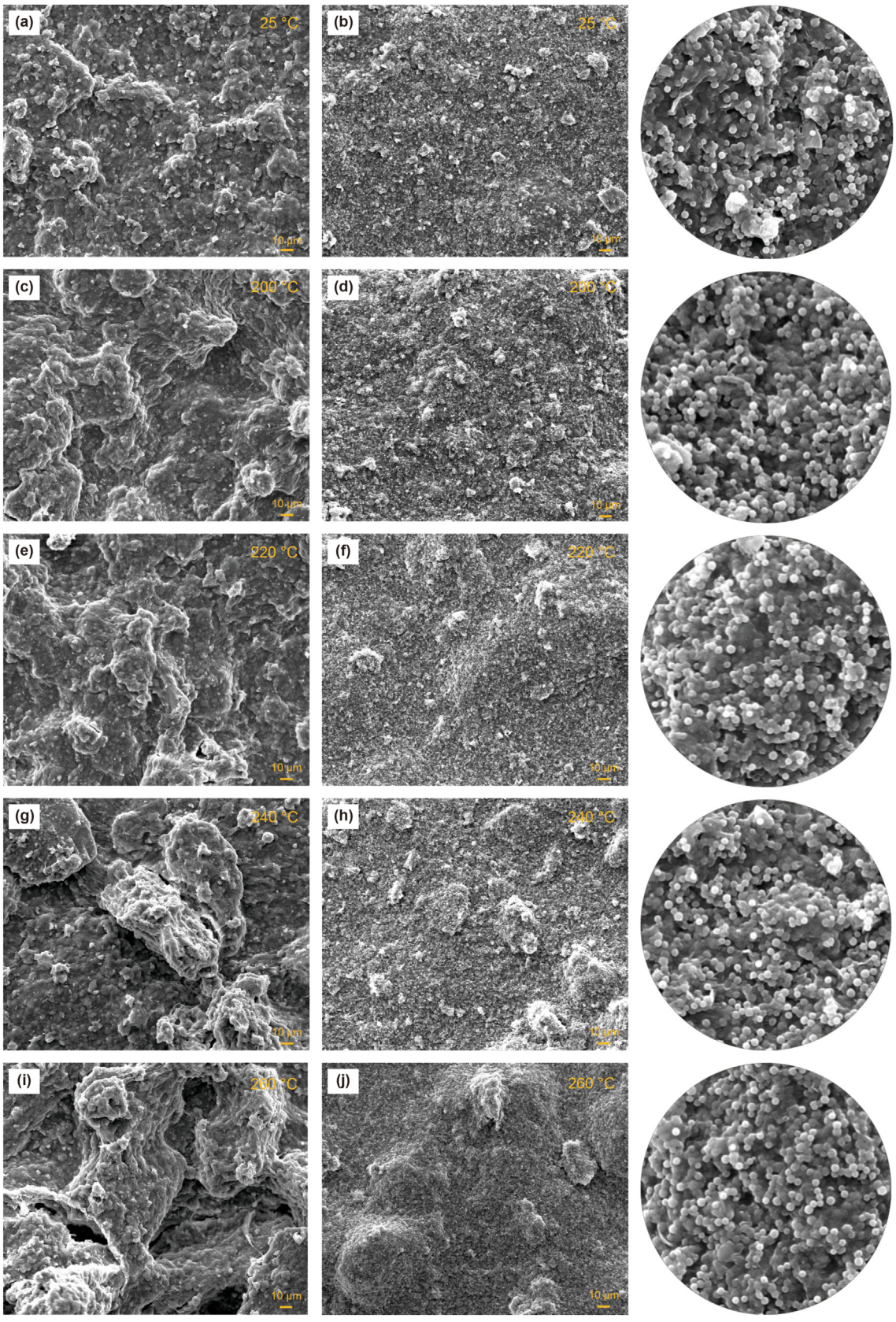

Fig. 16. Microscopic morphology of mud cake.

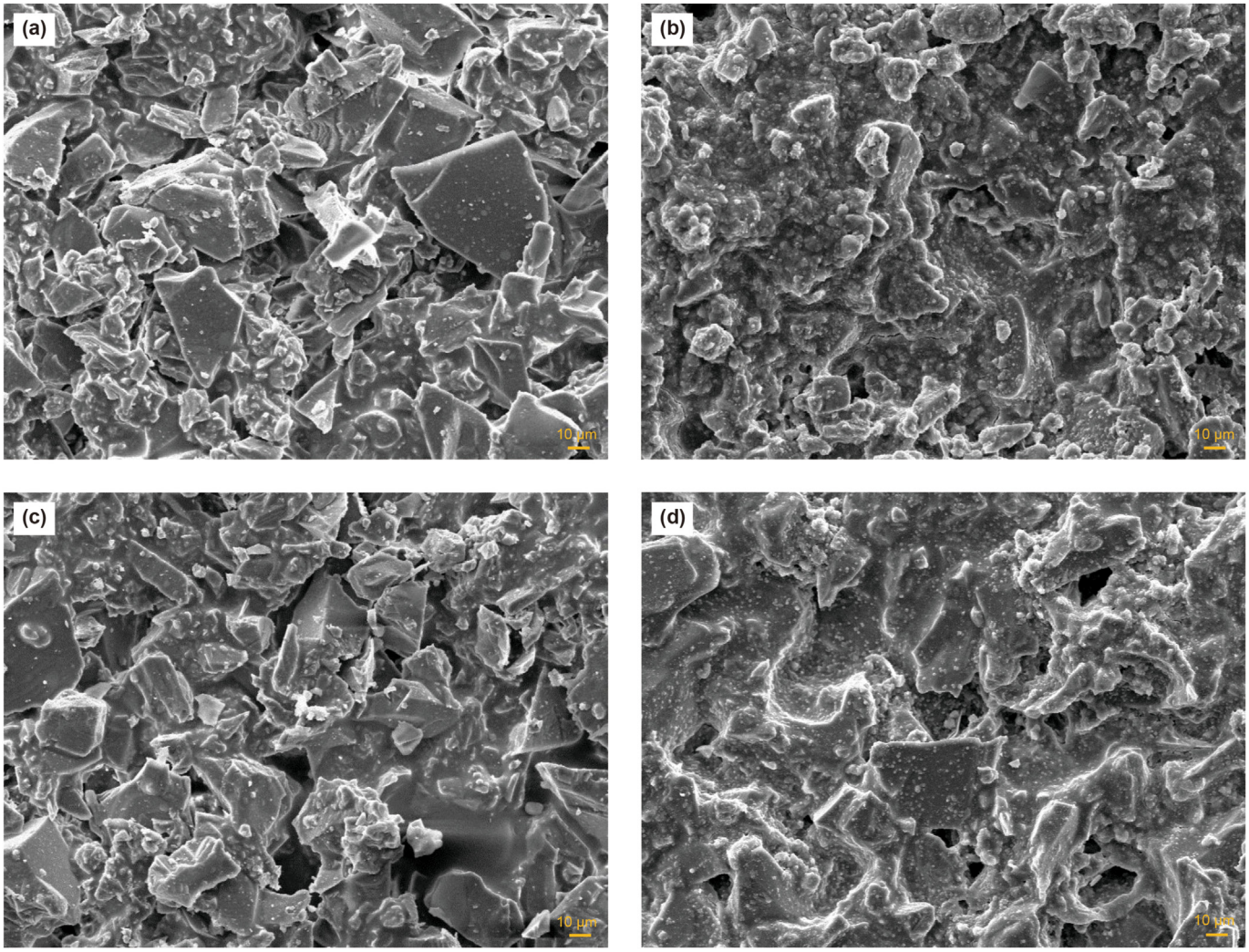

Fig. 17. Microscopic morphology of sand disc. (**a**) sand disc (3 μm) before blocking; (**b**) sand disc (3 μm) after blocking; (**c**) sand disc (5 μm) before blocking; (**d**) sand disc (5 μm) after blocking.

sealing layer and preventing infiltration of filtrate. In contrast to silica, strongly adsorbing rigid blocking agents not only rely on particle bridging, but also have an adsorption effect. At the same time, QW-1 can participate in the formation of mud cake inside and outside the well wall.

4. Conclusion

In this study, a high temperature resistant strong adsorption rigid blocking agent (QW-1) was prepared by grafting amide groups and quaternary ammonium groups on the surface of KH570 modified silica. TGA experiments show that QW-1 has good thermal stability, and the initial decomposition temperature is as high as 247 °C. It has good application prospect in high temperature resistant and strong blocking water-based drilling fluid system. Meanwhile, the average particle size of QW-1 is 1.46 μm, and the water contact angle is 10.5°, which has strong hydrophilicity and can be well dispersed in water. The experimental results showed that when 2 wt% QW-1 was added to recipe A (4 wt% bentonite slurry+0.5 wt% DSP-1), the API filtration loss decreased from 7.8 to 6.4 mL. After aging at 240 °C, the API filtration loss was reduced from 21 to 14 mL, which has a certain performance of high temperature reduction of filtration loss, and has a certain performance of salt resistance. At the same time, the sealing effect is good for 80–100 mesh and 100–120 mesh sand beds as well as 3 and 5 μm ceramic sand discs, indicating that QW-1 can be effective in sealing conventional cracks and pores as well as tiny cracks and pores. In addition, the mechanism of action of QW-1 was further investigated. The results show that QW-1 with amide and quaternary ammonium groups on the molecular chain can be adsorbed onto the surface of clay particles through hydrogen bonding and electrostatic interaction to form a dense blocking layer, thus preventing further intrusion of drilling fluid into the formation. In conclusion, the research of high temperature resistant and strong adsorption rigid blocking agent is of great significance to the safe and efficient development of ultra-deep and ultra-deep oil and gas resources.

Data availability statement

All data that support the findings of this study are included in this manuscript and its supplementary information files.

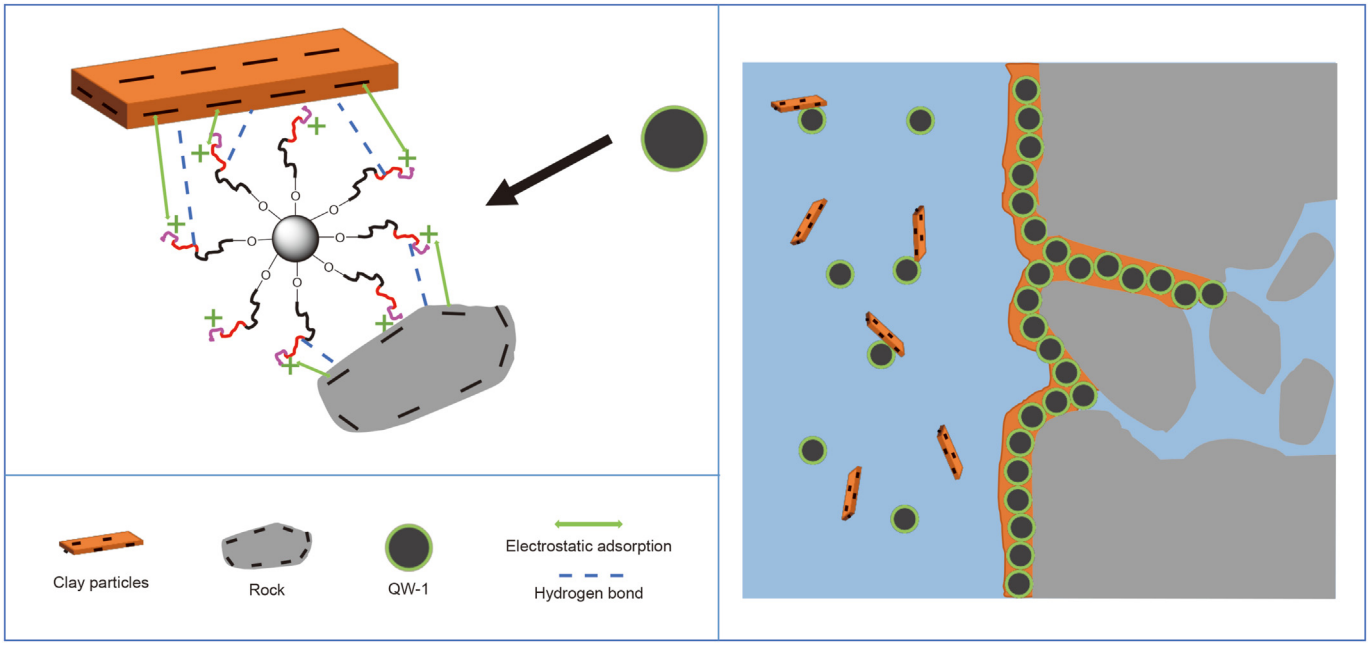

Fig. 18. Schematic diagram of blocking mechanism of QW-1.

CRediT authorship contribution statement

Zhe Xu: Writing – original draft, Visualization, Supervision, Methodology, Investigation, Formal analysis. **Jin-Sheng Sun:** Writing – review & editing, Supervision, Funding acquisition. **Jing-Ping Liu:** Supervision, Funding acquisition, Formal analysis, Writing – review & editing. **Kai-He Lv:** Formal analysis, Writing – review & editing. **Xiao-Dong Dong:** Validation. **Zong-Lun Wang:** Validation. **Tai-Feng Zhang:** Validation. **Yuan-Wei Sun:** Validation. **Zhi-Wen Dai:** Validation.

Declaration of competing interest

The authors declare that they have no known competing financial interests or personal relationships that could have appeared to influence the work reported in this paper.

Acknowledgments

This work was supported by the National Natural Science Foundation of China (No. 52074330, No. 52288101).

References

Ao, T., Yang, L.L., Xie, C.L., et al., 2021. Zwitterionic silica-based hybrid nanoparticles for filtration control in oil drilling conditions. ACS Appl. ACS Applied Nano Materials 4 (10), 11052–11062. https://doi.org/10.1021/acsanm.1c02504.

Bai, X.D., Yong, X.M., Koutsos, V., et al., 2021. Dispersive and filter loss performance of calcium carbonate nanoparticles in water for drilling fluid applications. Nanotechnology 32 (48), 485704. https://doi.org/10.1088/1361-6528/ac1dd2.

Boyou, N.V., Ismail, I., Sulaiman, W.R.W., et al., 2019. Experimental investigation of hole cleaning in directional drilling by using nano-enhanced water-based drilling fluids. J. Petrol. Sci. Eng. 176, 220–231. https://doi.org/10.1016/j.petrol.2019.01.063.

Cescon, L.d.S., Quartarone, P., Ribeiro, S.P.d.S., et al., 2018. Cationic starch derivatives as reactive shale inhibitors for water-based drilling fluids. J. Appl. Polym. Sci. 135 (33), 46621, 1012/ap.46621.

Dong, T.F., Jiang, G.C., He, Y.B., et al., 2023. A novel low molecular quaternary polymer as shale hydration inhibitor. J. Mol. Liq. 370 (15), 120934. https://doi.org/10.1016/j.molliq.2022.120934.

Dong, W.X., Pu, X.L., Ren, Y.J., et al., 2019. Thermoresponsive bentonite for water-based drilling fluids. Materials 12 (13), 2115. https://doi.org/10.3390/ma12132115.

Dong, X.D., Sun, J.S., Huang, X.B., et al., 2022. Synthesis of a low-molecular-weight filtrate reducer and its mechanism for improving high temperature resistance of water-based drilling fluid gel system. Gels 8 (10), 619. doi:10.3390/gels8100619.

Feng, W.P., Wang, F.Y., Jiang, T., et al., 2020. Origin and accumulation of petroleum in deep precambrian reservoir in Baxian Sag, Bohai Bay basin, China. Mar. Petrol. Geol. 120 (1), 104541. https://doi.org/10.1016/j.marpetgeo.2020.104541.

Gautam, S., Guria, C., Rajak, V.K., 2022. A state of the art review on the performance of high-pressure and high-temperature drilling fluids: towards understanding the structure-property relationship of drilling fluid additives. J. Petrol. Sci. Eng. 213, 110318. https://doi.org/10.1016/j.petrol.2022.110318.

Guo, X.S., Hu, D.F., Huang, R.C., et al., 2020. Deep and ultra-deep natural gas exploration in the Sichuan Basin: progress and prospect. Nat. Gas. Ind. B 7 (5), 419–432. https://doi.org/10.1016/j.ngib.2020.05.001.

Hoxha, B.B., Van, E.O., Daigle, H., 2019. How do nanoparticles stabilize shale? SPE Drill. Complet. 34 (2), 143–158. https://doi.org/10.2118/184574-pa.

Ismail, A.R., Aftab, A., Ibupoto, Z.H., et al., 2016. The novel approach for the enhancement of rheological properties of water-based drilling fluids by using multi-walled carbon nanotube, nanosilica and glass beads. J. Petrol. Sci. Eng. 139, 264–275. https://doi.org/10.1016/j.petrol.2016.01.036.

Jia, X.R., Zhao, X.H., Chen, B., et al., 2022. Polyanionic cellulose/hydrophilic monomer copolymer grafted silica nanocomposites as HTHP drilling fluid-loss control agent for water-based drilling fluids. Appl. Surf. Sci. 578 (15), 152089. https://doi.org/10.1016/j.apsusc.2021.152089.

Jiang, J., Wang, W., Shen, H.Y., et al., 2017. Characterization of silica particles modified with γ-methacryloxypropyltrimethoxysilane. Appl. Surf. Sci. 397 (1), 104–111. https://doi.org/10.1016/j.apsusc.2016.11.075.

Kök, M.V., Bal, B., 2019. Effects of silica nanoparticles on the performance of water-based drilling fluids. J. Petrol. Sci. Eng. 180, 605–614. https://doi.org/10.1016/j.petrol.2019.05.069.

Li, D.Q., Pang, S.C., Xuan, Y., et al., 2023. Nano-grafted acrylamide copolymer as an anti-temperature and anti-calcium fluid loss agent for water-based drilling fluids. Energy & Fuels 37 (10), 7213–7220. https://doi.org/10.1021/acs.energyfuels.3c00919.

Liu, F., Yao, H.L., Liu, Q.X., et al., 2021. Nano-silica/polymer composite as filtrate reducer in water-based drilling fluids. Colloids Surf. A Physicochem. Eng. Asp. 627 (20), 127168. https://doi.org/10.1016/j.colsurfa.2021.127168.

Luo, Y.H., Lin, L., Luo, P.Y., et al., 2023. Polymer nanocomposite ADA@SM as a high-temperature filtrate reducer for water-based drilling fluids and its filtration loss mechanism. Colloids Surf. A Physicochem. Eng. Asp. 672, 131701. https://doi.org/10.1016/j.colsurfa.2023.131.701.

Lou, R.X., Wang, L.W., Wang, L.X., et al., 2022. Characteristics of fluid inclusions and hydrocarbon accumulation period of Huoshiling-Yingcheng Formations in

Wangfu fault depression. Songliao Basin, China. J. Petrol. Sci. Eng. 208, 109421. https://doi.org/10.1016/j.petrol.2021.109421.
Luz, R.C.S.d., Paixão, M.V.G., Balaban, R.d.C., 2019. Nanosilica-chitosan hybrid materials: preparation, characterization and application in aqueous drilling fluids. J. Mol. Liq. 279 (1), 279–288. https://doi.org/10.1016/j.molliq.2019.01.131.
Mao, H., Qiu, Z.S., Shen, Z.H., et al., 2015. Novel hydrophobic associated polymer based nano-silica composite with core-shell structure for intelligent drilling fluid under ultra-high temperature and ultra-high pressure. Prog. Nat. Sci.: Mater. Int. 25 (1), 90–93. https://doi.org/10.1016/j.pnsc.2015.01.013.
Martin, C., Babaie, M., Nourian, A., et al., 2023. Designing Smart drilling fluids using modified nano silica to improve drilling operations in Geothermal wells. Geothermics 107, 102600. https://doi.org/10.1016/j.geothermics.2022.102600.
Shen, Y., Zhu, Y.Q., Gao, Z.J., et al., 2023. Nano-SiO_2 grafted with temperature-sensitive polymer as plugging agent for water-based drilling fluids. Arabian J. Sci. Eng. 48, 9401–9411. https://doi.org/10.1007/s13369-022-07486-x.
Sun, C.L., Li, G.C., Sun, Y.T., et al., 2019. Modelling hydration swelling and weakening of montmorillonite particles in mudstone. Processes 7 (7), 428. https://doi.org/10.3390/pr7070428.
Sun, J.S., Wang, Z.L., Liu, J.P., et al., 2022. Notoginsenoside as an environmentally friendly shale inhibitor in water-based drilling fluid. Petrol. Sci. 19 (2), 608–618. https://doi.org/10.1016/j.petsci.2021.11.017.
Villada, Y., Busatto, C., Casis, N., et al., 2022. Use of synthetic calcium carbonate particles as an additive in water-based drilling fluids. Colloids Surf. A Physicochem. Eng. Asp. 652, 129801. https://doi.org/10.1016/j.colsurfa.2022.129801.
Wang, H.G., Huang, H.C., Bi, W.X., et al., 2022. Deep and ultra-deep oil and gas well drilling technologies: progress and prospect. Nat. Gas. Ind. B 9 (2), 141–157. https://doi.org/10.1016/j.ngib.2021.08.019.
Wang, Y.T., Xiao, M.Q., Chen, C.W., et al., 2023. Preparation and performance study of the self-brittle composite detergent with controllable morphology for radioactive decontamination of surface layer of various materials by RAFT one-pot synthesis. React. Funct. Polym. 187, 105591. https://doi.org/10.1016/j.reactfunctpolym.2023.105591.
Wang, Z.L., Liu, J.P., Lv, K.H., et al., 2023. Hydrophobically modified low molecular weight polymers as high temperature resistant shale inhibitor. J. Mol. Liq. 382 (15), 121856. https://doi.org/10.1016/j.molliq.2023.121856.
Xu, K., Yang, H.J., Zhang, H., et al., 2022. Fracture effectiveness evaluation in ultra-deep reservoirs based on geomechanical method, Kuqa Depression, Tarim Basin, NW China. J. Petrol. Sci. Eng. 215, 110604. https://doi.org/10.1016/j.petrol.2022.110604.
Xu, Z., Sun, J.S., Li, L., et al., 2023. Development and performance evaluation of a high temperature resistant, internal rigid, and external flexible plugging agent for water-based drilling fluids. Petroleum 9 (1), 33–40. https://doi.org/10.1016/j.petlm.2022.07.004.
Yi, H., Zhang, X., Zhao, Y.L., et al., 2016. Molecular dynamics simulations of hydration shell on montmorillonite (001) in water. Surf. Interface Anal. 48 (9), 976–980. https://doi.org/10.1002/sia.6000.
Yu, F.Y., Gao, J., Liu, C.P., et al., 2020. Preparation and UV aging of nano-SiO_2/fluorinated polyacrylate polyurethane hydrophobic composite coating. Prog. Org. Coating 141, 105556. https://doi.org/10.1016/j.porgcoat.2020.105556.
Yu, P.Z., 2015. Modification of waste polyacrylonitrile fiber and its application as a filtrate reducer for drilling. Petrol. Sci. 12, 325–329. https://doi.org/10.1007/s12182-015-0019-8.